Taylor & Francis
Taylor & Francis Group

Biofouling
The Journal of Bioadhesion and Biofilm Research

ISSN: 0892-7014 (Print) 1029-2454 (Online) Journal homepage: www.tandfonline.com/journals/gbif20

Metabarcoding and metabolomics offer complementarity in deciphering marine eukaryotic biofouling community shifts

Jean-François Briand, Xavier Pochon, Susanna A. Wood, Christine Bressy, Cédric Garnier, Karine Réhel, Félix Urvois, Gérald Culioli & Anastasija Zaiko

To cite this article: Jean-François Briand, Xavier Pochon, Susanna A. Wood, Christine Bressy, Cédric Garnier, Karine Réhel, Félix Urvois, Gérald Culioli & Anastasija Zaiko (2018) Metabarcoding and metabolomics offer complementarity in deciphering marine eukaryotic biofouling community shifts, Biofouling, 34:6, 657-672, DOI: 10.1080/08927014.2018.1480757

To link to this article: https://doi.org/10.1080/08927014.2018.1480757

BIOFOULING, 2018
VOL. 34, NO. 6, 657–672
https://doi.org/10.1080/08927014.2018.1480757

Taylor & Francis
Taylor & Francis Group

Metabarcoding and metabolomics offer complementarity in deciphering marine eukaryotic biofouling community shifts

Jean-François Briand[a], Xavier Pochon[b,c], Susanna A. Wood[b], Christine Bressy[a], Cédric Garnier[d], Karine Réhel[e], Félix Urvois[a], Gérald Culioli[a] and Anastasija Zaiko[b,c]

[a]Université de Toulon, MAPIEM-EA 4323, Toulon, France; [b]Coastal and Freshwater Group, Cawthron Institute, Private Bag 2, Nelson 7042, New Zealand; [c]Institute of Marine Science, University of Auckland, Private Bag 349, Warkworth 0941, New Zealand; [d]Université de Toulon, PROTEE-EA 3819, Toulon, France; [e]Université de Bretagne Sud, LBCM-EA 3883, IUEM, Lorient, France

ABSTRACT

Metabarcoding and metabolomics were used to explore the taxonomic composition and functional diversity of eukaryotic biofouling communities on plates with antifouling paints at two French coastal sites: Lorient (North Eastern Atlantic Ocean; temperate and eutrophic) and Toulon (North-Western Mediterranean Sea; mesotrophic but highly contaminated). Four distinct coatings were tested at each site and season for one month. Metabarcoding showed biocidal coatings had less impact on eukaryotic assemblages compared to spatial and temporal effects. Ciliophora, Chlorophyceae or Cnidaria (mainly hydrozoans) were abundant at Lorient, whereas Arthropoda (especially crustaceans), Nematoda, and Ochrophyta dominated less diversified assemblages at Toulon. Seasonal shifts were observed at Lorient, but not Toulon. Metabolomics also showed clear site discrimination, but these were associated with a coating and not season dependent clustering. The meta-omics analysis enabled identifications of some associative patterns between metabolomic profiles and specific taxa, in particular those colonizing the plates with biocidal coatings at Lorient.

ARTICLE HISTORY
Received 22 December 2017
Accepted 18 May 2018

KEYWORDS
macrofouling; eukaryotes; marine biofilms; 18S rRNA gene; physico-chemical; parameters; artificial surfaces

Introduction

Marine biofouling organisms colonize immersed surfaces and form communities on diverse biogenic habitats. This colonization process is most intense in coastal or shallow waters, where species diversity, temperatures, nutrient levels, and availability of submerged substrata are usually higher compared to offshore areas (e.g. Railkin 2004). Many thousands of taxa have been identified in marine biofouling, including bacteria, algae, and invertebrate phyla. Despite the extensive literature on biofouling, including those addressing antifouling (AF) effects (e.g. Dürr & Thomason 2010), very few publications have described the macrofouling communities to genus or species level, and the majority have only considered the most predominant taxa. Temporal and spatial fouling assemblages have mostly been studied on static artificial substrata e.g. pilings and pontoons (Connell 2001), artificial reefs (Brown 2005) or aquaculture cages (Braithwaite & McEvoy 2004).

Despite similar taxonomic groups have been reported from marine biofouling in both temperate and tropical areas, the structure of the communities often varies depending on ambient factors, such as substrate type, water currents, seasonal environmental variations, and vertical habitat zonation (Wood et al. 2000, Brown et al. 2003). For example, photosynthetic fouling biomass is usually limited to well-irradiated areas whereas barnacle larvae are typically found to be negatively phototrophic (Hanson & Bell 1976, Railkin 2004). Some authors have demonstrated that mussel colonization requires precursory fouling by other species or that macrofouling assemblages converge with time regardless of the nature of reefs (Brown 2005). However, the presence of many phylogenetically different organisms all growing together often impedes highly resolved taxonomic identification, hence limiting the identification of the key environmental factors determining patterns in biofouling communities.

The use of molecular high-throughput sequencing approaches (e.g. metabarcoding, Taberlet et al. 2012) has recently been applied to unravel the composition and structure of eukaryotic macrofouling assemblages (Pochon et al. 2013, Leary et al. 2014, Pochon et al.

CONTACT Jean-François Briand briand@univ-tln.fr
Supplemental material for this paper is available online at https://doi.org/10.1080/08927014.2018.1480757

2015, Sanli et al. 2015, Sathe et al. 2017). In addition, Zaiko et al. (2016) showed that traditional and molecular approaches were consistent at high taxonomic levels, but that metabarcoding was able to identify many more taxa at the genera/species level. In addition to improving biodiversity assessments of macrofouling assemblages, these approaches have a great potential for resolving challenges associated with traditional taxonomic identification (e.g. the identification of cryptic species or early life stages).

Metabolomics is an emerging approach in the omics sciences, and its application to determine the metabolic production of complex aquatic communities has been limited (e.g. Beale et al. 2013, Brauer et al. 2015, Gutarowska et al. 2015). This approach can provide valuable information on functional community composition and biofilm responses to specific environmental conditions or colonized surface properties. By integrating meta-omics approaches, new functional insights of marine biofilm communities can be unravelled, enabling improved predictions of the spatial and temporal evolution in these highly complex biological systems.

In this study, a combined approach was used incorporating metabarcoding, traditional visual inspection, and metabolomics to provide complementary information on biofouling communities, including coverage data, molecular taxonomy, and functional diversity. The objectives of the present study were to characterize eukaryotic assemblages colonizing artificial surfaces coated with different AF formulations, and to assess effects of seasonal variation over a one-year cycle at two environmentally contrasting locations on the French coasts: (*i*) a temperate and eutrophic site on the Atlantic coasts of Brittany (Lorient), and (*ii*) a mesotrophic but highly contaminated site in the North-Western Mediterranean Sea (Toulon).

Materials and methods

Sites, coatings and immersion

Two sites were selected in France: Lorient Bay (South coast of Brittany, Atlantic Ocean) at Kernevel marina (47°43'8"N, 3°22'7"W; Figure S1), and Toulon Bay (North-Western Mediterranean Sea) in a semi-enclosed pond in a military harbour (43°06'25"N; 5°55'41"E).

Four different artificial substrata (Table S2) were used including bare but sandblasted poly(vinyl)chloride (PVC) as a reference (R), and three AF coatings. The latter were prepared using the same commercial binder (Neocryl® B-725), but each differed in their biocide composition (5% of the final wet weight): zinc ethylene-bis-dithiocarbamate or Zineb® (I), zinc pyrithione (Z), and copper pyrithione (C). The first biocide was provided by Agrica S.A. (Bulgaria) and the copper and zinc pyrithiones by Arch UK Biocides (UK).

Panels (5 × 5 cm) were prepared in triplicate for each of the four seasons (Winter = Wi, Spring = Sp, Summer = Su, Autumn = Au) at the two sites, which corresponded to 96 panels for each of the two approaches (metabarcoding and metabolomics). AF paints were applied on both sides of the sandblasted PVC panels using a bar-coater of 300 µm, before drying for fifteen days prior to immersion.

Panels were submerged vertically at 1 m depth using a static permanent raft at Toulon and non-permanent PVC frames fixed on a pontoon at Lorient for one month at each season at each site (Table S3). Environmental data (temperature, salinity, pH, oxygen, nutrients and metals) are described in Briand et al. (2017) (Table S4).

DNA extraction, 18S rRNA gene amplification and high-throughput sequencing

After immersion for month, 96 panels were scraped and the material isolated for DNA extraction, which was performed on all samples using a Power Soil DNA Isolation kit (Qiagen, Courtaboeuf, France), following the manufacturer's instructions (Camps et al. 2014). Triplicate DNA extracts were pooled and a two-step tailed PCR amplicon procedure (Pramanik and Li 2002) employed for generating an Illumina MiSeq™ library for the 32 samples. The universal primers Uni18SF (5'-AGGGCAAKYCTGGTGCCAGC-3') and Uni18SR (5'-GRCGGTATCTRATCGYCTT-3') (Zhan et al. 2013) were used to amplify the eukaryotic V4 region of the nuclear small subunit ribosomal RNA (18S rRNA) gene. The primers for the first PCR were modified to include Illumina™ overhang adaptors as described in (Kozich et al. 2013). PCR amplifications were undertaken on an Eppendorf Mastercycler (Eppendorf, Germany) in a total volume of 30 µl using AmpliTaq Gold® 360 PCR Master Mix (Life Technologies, USA), 1 µl of each primer (10 µM, IDT DNA, USA) and 1 µl of template DNA. Reaction cycling conditions were: 94 °C for 3 min, followed by 25 cycles of 94 °C for 45s, 55 °C for 45s, 72 °C for 2 min, and a final extension of 72 °C for 5 min.

Amplicons were purified using the AMPure™ XP system (Agencourt, USA), and quantified using the QuBit BR dsDNA kit (Invitrogen, USA), diluted to a concentration of 1 ng/µL and sent to New Zealand

Genomics Limited (University of Auckland, New Zealand) for final library preparation. Sequencing adapters and sample-specific indices were added to each amplicon via a second round of PCR using the Nextera™ Index kit (Illumina™). Amplicons were pooled into a single library and paired-end sequences (2 × 250) generated on a MiSeq instrument using the TruSeq™ SBS kit (Illumina™). Sequence data were automatically demultiplexed using MiSeq Reporter (v2), and forward and reverse reads assigned to samples.

Bioinformatics

Bioinformatic analysis of metabarcoding data was performed using MOTHUR v.1.34.4 (Schloss et al. 2009). Forward and reverse paired-end sequences were assembled independently for each sample. The bioinformatics pipeline and analysis procedure described in Kozich et al. (2013) was applied as described below.

Overlapped raw sequence reads were denoised, trimmed and filtered prior to downstream analyses (settings applied for screen.seq command were: minoverlap = 25, maxambig = 0, minlength = 430, maxhomop = 8). The retained sequences were de-replicated into unique sequences and aligned against the reference SILVA 123 database for eukaryotic rRNA sequences (Quast et al. 2013). PCR-mediated recombination in amplification products (i.e. chimeras) were identified and removed from the dataset using the UCHIME algorithm (Edgar et al. 2011) both in *de novo* and dataset modes.

Sequence reads from each sample were clustered into Operational Taxonomic Units (OTUs) at 97% similarity. OTUs represented by less than ten sequences over the dataset were discarded. The remaining OTUs were taxonomically assigned using the Protist Ribosomal 2 (PR2) database (Guillou et al. 2013). For taxonomic classification, the Wang method was applied with minimum bootstrap value set at 97% (Wang et al. 2007). The taxonomic nomenclature of assignments was verified against the World Register of Marine Species, AlgaeBase, Encyclopedia of Life and Integrated Taxonomic Information System databases. The taxonomic data were screened thoroughly to eliminate taxa unlikely to be present within biofouling assemblages (e.g. terrestrial plant species). The retained dataset of assigned taxa (at the lowest level) and records of the number of sequences per sample were used for biodiversity assessment and statistical analyses.

All raw sequences were deposited at NCBI BioProject database (https://www.ncbi.nlm.nih.gov/sra) under accession number SRP140577.

Determination of macrofouling assemblages based on visual inspection

Visual inspection was performed on the set of panels used for metabolomics immediately after retrieving them from the seawater and prior to sampling. This was undertaken for Toulon panels only (triplicates of four treatments at each season) and allowed identification and estimation of percent cover of the type of colonizers (biofilm, green, red or brown algae, and hard fouling such as encrusting bryozoans, tubewroms, spirorbis, and barnacles).

Liquid chromatography-mass spectrometry (LC-MS) metabolomic analysis

Immediately after retrieval, the second set of 96 panels was frozen (−20 °C). Each frozen panel was then scrapped with a scalpel to recover all the biological material from its surface. A mixture of methanol (MeOH)/dichloromethane (DCM) (25 ml, 1:1, *v*/*v*) was added to the sampled biological matrix. The resulting solution was sonicated (ultrasonic bath, 10 min at 20 °C), mixed with 500 mg of C_{18} silica powder (Phenomenex, Torrance, CA, USA) and vacuum-concentrated. The dried powder was deposited on a solid phase extraction cartridge (Strata C18-e, 2g, 55 µm, Phenomenex), pre-conditioned (10 ml, MeOH) and conditioned (10 ml, H_2O). The dried extract was desalted (10 ml, H_2O) and eluted (10 ml, MeOH/DCM, 1:1, *v*/*v*) and then 10 ml of DCM. The resulting organic extracts were then concentrated under reduced pressure, re-suspended in MeOH (1 ml) and stored at -20 °C in a 2-ml high performance-liquid chromatography (HPLC) vial before further analyses.

Chromatographic analyses were performed on an Elite LaChrom system (VWR, Fontenay-sous-Bois, France) composed of a quaternary pump equipped with an online degasser (L-2130), an autosampler including an injection system with variable volume (L-2200) and a column oven (L-2300). Separations were performed on an analytical reversed-phase column (Gemini C_6-Phenyl 5 µm, 250 × 3 mm, Phenomenex) equipped with a guard cartridge and maintained at 30 °C. The flow rate was set at 0.5 ml min^{-1} and the injected sample volume was 10 µl. The mobile phase consisted of H_2O (A) and acetonitrile (B) containing both 0.1% of formic acid. The elution gradient started at

90% A for 5 min, increasing to 100% B in 30 min with a final isocratic step for 20 min; before returning to 90% A in 1 min which was maintained for a further 9 min. The chromatographic system was coupled with an ion trap electrospray ionization mass spectrometer (Esquire 6000, Bruker Daltonics, Wissembourg, France). The operating conditions for the electrospray interface were set as follows: nebulizing gas (nitrogen (N_2) pressure: 3.45 bars, drying gas (N_2) flow: 12 l min^{-1}, drying temperature: 350 °C, capillary voltage: 4000 V. Mass spectra were acquired in the full scan mode with *m/z* from 50 to 1200 and a maximum filling time of 200 ms. Data were handled with Data Analysis v. 4.3 (Bruker Daltonics).

Liquid Chromatography – Mass Spectrometry (LC-MS) raw data were converted into netCDF files and preprocessed with XCMS v. 1.38.0 under R 3.1.0 environment. Peak picking was performed with the *matchedFilter* method using the following parameters: *snthresh* = 5, retention time correction with the obiwarp method (*profstep* = 0.1), peak grouping with *bw* = 5 and *mzwidth* = 0.5, gap filling with default parameters. A filtering step based on an in-house script on R was used to remove signals observed in blank samples (signal/noise ration >10).

Statistical analyses

The untransformed metabarcoding data (number of reads per OTU per sample) were used to generate OTU rarefaction curves for each treatment using R software vegan package (Oksanen et al. 2014).

The univariate effect of three factors (AF coating, location, and season) on species richness (assessed as number of taxa at lowest taxonomic level assigned) was assessed by applying a generalized linear mixed model (GLMM) implemented in R software lme4 package (Bates et al. 2015). In the models, treatment and location were used as fixed explanatory variables and season – as a random effect.

The multivariate differences in biofouling community composition between factors were assessed using distance-based permutational analysis (PERMANOVA, (Anderson 2001) implemented in PRIMER 7. AF coating and location were included as fixed factors, and season was treated as a random effect nested within location. Analysis was based on Jaccard resemblance measure using presence-absence data (taxonomic assignments at the lowest level). This approach was also applied for the non–metric multidimensional analysis (NMDS) and considered appropriate to account for possible biases associated with the limited quantification capacity of eukaryotic metabarcoding (Kelly et al. 2014). Canonical correspondence analyses (CCA) linking environmental parameters and communities (using the Jaccard index) were performed using CANOCO®. The communities were considered at the class level to get a reasonable number of variables. To identify potential resistance or sensitivity of OTUs to AF coatings, the ratio between the relative abundance for C, Z or I and R was considered for each OTU independently and at each site (mean of the four seasons). OTUs with the ratio lower than 0.5 were considered as sensitive and those higher than two as resistant.

For the visual assessment data from Toulon panels, principal component analysis (PCA) was performed using XLSTAT® software. PERMANOVA was also undertaken on Bray-Curtis similarity matrix after square root transformation of original percentage cover data. The PERMANOVA design included AF formulation and season as fixed and random factors, respectively, with a post-hoc pair-wise test applied to the AF formulation factor.

Partial least squares discriminant analyses (PLS-DA) were undertaken on the LC-MS-based metabolomics data using the MetaboAnalyst 3.0 online resource (http://www.metaboanalyst.ca).

Results

Taxonomic diversity - high-throughput sequencing data

The V4 region of 18S rRNA gene was successfully amplified from all 32 samples. High-throughput sequencing produced 1,037,511 raw sequences with an average length of 469 base pairs. The stringent filtering and chimera checks resulted in removal of 64% of sequence reads. After clustering of 151,247 unique sequences and removal of rare OTUs, 184,110 reads were retained for downstream analyses.

Most of the sequences (99.9%, $n = 183{,}935$) were taxonomically assigned against the PR2 database to the supergroup or lower taxonomic level at 97% similarity. Only 15 sequences were assigned to a non-marine organism and were discarded. One sample (T14: TAuZ) produced only 226 high-quality reads and was removed from the subsequent analyses. As indicated by the rarefaction curves (Figure S5), the other samples were adequately sequenced for the biodiversity assessment. From the retained dataset, 81% of sequences were assigned to metazoans, 17% to protists, and 2% to algal and plant taxa. Overall, arthropods were the dominant group of organisms

comprising 46% of the sequence reads, followed by cnidarians (22%).

Species richness and variability determined from the panels deployed in Lorient was on average higher than that in Toulon (19 ± 7 and 13 ± 3 species, for Lorient and Toulon, respectively; Figure S6). As evidenced by the fitted GLMM model ($R^2 = 0.5$; goodness-of-fit r = 0.7, $p < 0.001$), among tested factors (AF coating, location and season) only location had a significant effect on species richness ($F = 8.808$, $p = 0.007$, Table 1).

A marked partitioning of phyla was observed between the two locations (Figure 1), with the dominance of ciliates and cnidarians in Lorient samples and arthropods and nematodes in Toulon samples. A clear seasonal shift in assemblages was also identified (Figure 1), while the effect of AF coating on the community structure was not evident at higher taxonomic levels. The PERMANOVA analysis confirmed that location and season were the most important factors which determined the community composition (Table 2). The multivariate analysis (OTU data, NMDS) indicated that seasonal variation in community composition was more apparent in Lorient than in Toulon (Figure 2). Overall, eukaryotic assemblages on panels immersed in Lorient were more variable than those from Toulon (Figure 2).

The relative abundance of the most frequent eukaryotic OTUs revealed on the reference panels (R), including both non-specific (i.e. OTUs detected at both sites across more than three seasons), and site-specific OTUs (i.e. detected across more than two seasons at only one site), are shown in Figure 3 and Figure S7. Five OTUs were considered as frequent and non-specific. OTU 106 corresponded to the copepod *Harpacticus* sp. (Arthropoda, Crustacea) and was recorded throughout the year at the two sites without a clear seasonal trend. An unclassified Maxillopoda (Arthropoda, Crustacea, OTU 115) was recorded mainly during spring and summer at Toulon whereas no clear trend was observed at Lorient (Figure 3

Table 1. Results of the GLMM (χ^2 analysis of random effects and ANOVA for fixed effects) for the applied formula AF treatment + location + location × treatment+(1season).

Random effects:	Chi.sq	Chi.DF	Elim.num	*p* value		
Season	1.46	1	1	0.2		
Fixed effects: Analysis of variance table						
	Df	SumSq	MeanSq	F value	Pr(>F)	
Antifouling treatment	3	79.49	26.50	0.7181	0.5513	ns
Location	1	325.00	325.00	8.8080	0.0068	**
Treatment: location	3	33.81	11.27	0.3055	0.8211	ns
Residuals	23	848.67	36.90			

Signification code: '**' 0.01.

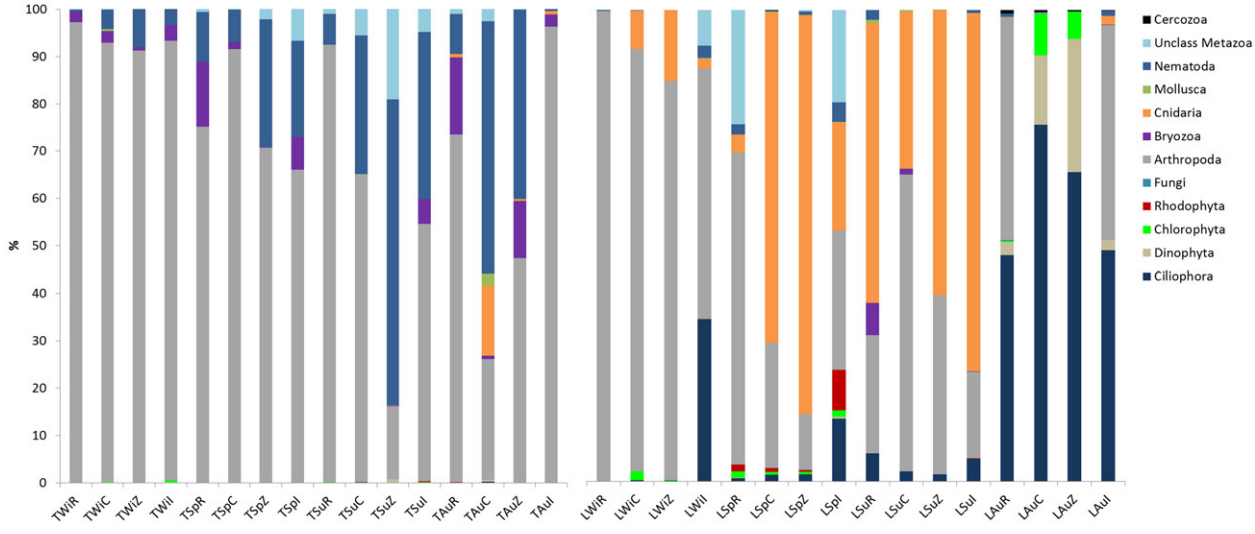

Figure 1. Relative abundance of higher taxa (% of sequence reads) between different experimental factors in the two study locations: Toulon and Lorient (France). L = Lorient, T = Toulon, Winter = Wi, Spring = Sp, Summer = Su, Autumn = Au, R = reference plates with no coating, I = plates coated with commercial binder (Neocryl® B-725) and Zineb®, C = plates coated with commercial binder (Neocryl® B-725) and copper pyrithione, Z = plates coated with commercial binder (Neocryl® B-725) and zinc pyrithione.

and Figure S7). Conversely, *Chromadorina* spp. (Nematoda, two OTUs, 153 and 154) were primarily recorded during spring and summer at Lorient and showed no clear pattern at Toulon. Finally, although the taxonomy of OTU 181 (Metazoa) could not be assigned, it was observed throughout the year at Toulon without marked variations, whereas its presence at Lorient was significantly higher during spring.

Five OTUs (2.6%) were recorded only at Toulon on R with an increase of the relative abundance in summer and autumn for four of them (OTU 98, Arthropoda, *Eudactylopus* sp.; OTU 104, Arthropoda, *Harpacticus* sp.; OTU 118, Arthropoda, Crustacea; OTU 172, Nematoda, Enoplea) (Figure 3 and Figure S7). Only OTU 166 (Nematoda, Chromadorea) showed a maximum occurrence in spring. Twenty OTUs (20.4%) were recorded only at Lorient with Ciliophora (14 OTUs): two dominant families, Zoothamniidae and Vorticellidae, included 12 OTUs displaying a similar pattern of increased relative abundance in summer and autumn (Figure 3 and Figure S7). In addition, Chlorophyta (two OTUs), Dinophyta, Cnidaria (three OTUs) and Arthropoda demonstrated a seasonal pattern in Lorient with higher relative abundances in spring and autumn.

A strong Spearman's rank pairwise correlation was observed between temperature and lead (Pb) ($r = 0.905$, $p = 0.005$, $n = 8$) and dissolved inorganic carbon (DIC) ($r = 0.881$, $p = 0.007$, $n = 8$). A correlation was observed between nitrates, silicates ($r = 0.881$, $p = 0.007$, $n = 8$) and dissolved organic carbon (DOC) ($r = 0.876$, $p = 0.037$, $n = 8$). Consequently, tem-

Table 2. PERMANOVA table for the multivariate effects of antifouling coating, location and season on the biofouling community (presence-absence of taxa at the lowest assigned taxonomy level after 18S rRNA gene amplification).

PERMANOVA table of results

Source	df	SS	MS	Pseudo-F	P(perm) *P(MC)*	Unique perms
AF Treatment	3	5046	1682.1	1.1217	0.255	9871
Location	1	25304	25304	4.9152	0.001	280
Season (Location)	6	31142	5190.3	3.4611	<0.001	9833
Treatment × Location	3	5697	1899.3	1.2665	0.081	9844
Residual	17	25494	1499.6			
Total	30	93391				

Permutational (permutation of residuals under a reduced model) and Monte-Carlo (for location factor with low final number of permutations) *p* values applied to test for significance.

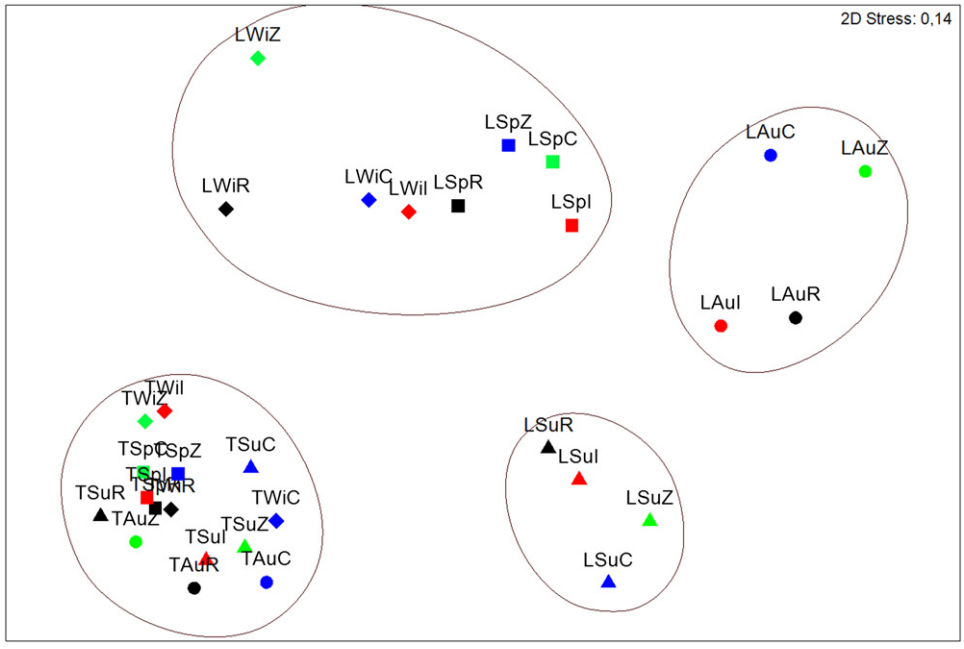

Figure 2. Non-metric Multi-Dimensional Scaling plot visualizing the differences in the detected biofouling communities depending on sites, seasons and coatings. The overlay lines indicate clusters at 20% similarity threshold. L = Lorient, T = Toulon/Winter = Wi, Spring = Sp, Summer = Su, Autumn = Au, R = reference plates with no coating, I = plates coated with commercial binder (Neocryl® B-725) and Zineb®, C = plates coated with commercial binder (Neocryl® B-725) and copper pyrithione, Z = plates coated with commercial binder (Neocryl® B-725) and zinc pyrithione.

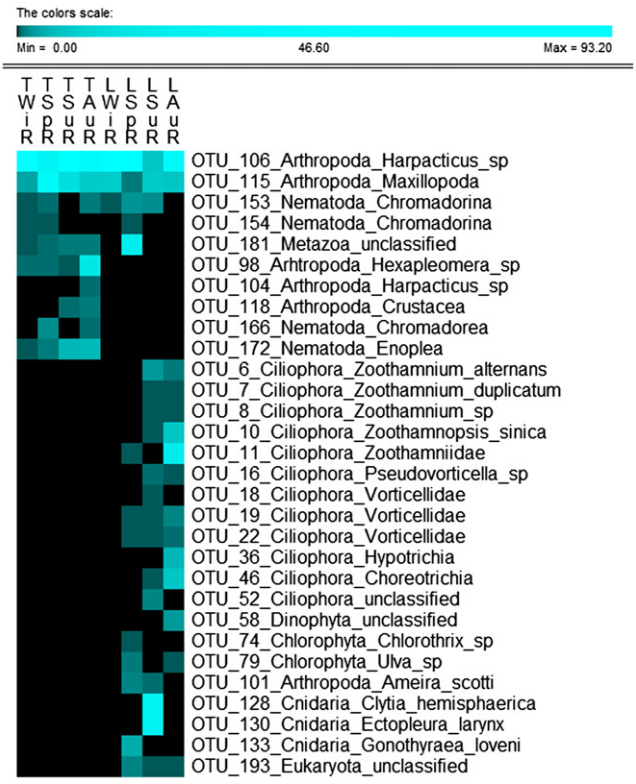

Figure 3. Heatmap of the relative abundance of the Operational Taxonomic Units (OTUs) characteristic of the eukaryotic communities at Toulon and Lorient on the reference plates (R = Poly(Vinyl)chloride only) during the four seasons. The figure shows only non-specific and frequent OTUs, i.e. at least at three seasons at both sites, and site specific, at least at two seasons at one site without any presence at the other. (L = Lorient, T = Toulon/Winter = Wi, Spring = Sp, Summer = Su, Autumn = Au)

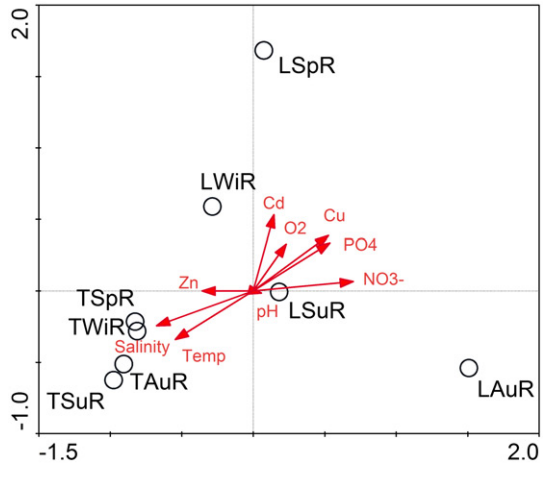

Figure 4. Canonical Correspondence Analysis of seawater environmental parameters and macrofouling assemblages on the reference plates at Toulon and Lorient. L = Lorient, T = Toulon, Winter = Wi, Spring = Sp, Summer = Su, Autumn = Au.

perature was chosen as a proxy for Pb and DIC, and nitrates for silicates and DOC for further CCA. Eukaryotic communities displayed two clusters depending on site (Figure 4). Communities at Toulon were clearly associated with high temperature, Pb and salinity. Conversely, communities at Lorient were significantly associated with high concentrations of nutrients (phosphates, nitrates and silicates), and DOC, but also copper (Cu) and cadmium (Cd). The cumulative percentage of variance of the species/environment relationship indicates that the first and second canonical axis explained 26.8% and 18.8%, respectively.

Impact of biocidal coatings on the eukaryotic community

Differentiating between OTUs resistance and tolerance to biocidal coatings was challenging, and it is acknowledged that inferences drawn from the current results remain hypothetical. Based on the eDNA signal from AF treated *vs* untreated (control) plates, seven Ciliophora OTUs were identified as resistant, as they were reported on most of the C or Z panels at Lorient (Figure 5). In the family Vorticellidae, resistance to both C and Z was observed. Conversely, two species from the genus *Holosticha* (Holostichadae) exhibited dissimilar resistance profiles (I for *H. bradburyae*, C for *H. diademata*). Among autotrophic taxa, Chlorophyta (OTU 74) and Dinophyta (OTU 58 and 61) appeared to be resistant to both C and Z at Lorient. However, Rhodophyta (OTU 82) colonized

specifically I panels at Lorient. *Mytilus edulis* (OTU 145), Nematoda (five OTUs) and a Platyhelminthes (from the order Rhabdocoela, OTU 177) were recorded only at Toulon with a specific resistance profile to C or Z, while two Nematoda (Chromadorina, OTU 154 and Enoplea, OTU 172), also colonized I panels.

Putatively sensitive OTUs were reported in the three other groups of Metazoa (Arthropoda, Bryozoa and Cnidaria). No particular pattern was observed among the six OTUs assigned to Arthropoda (Figure 5). The same OTUs exhibited resistant and/or sensitive profiles depending on the coating. For example, *Eudactylopus* (OTU 98) was resistant to I but sensitive to C in Toulon. *Harpacticus* sp. (OTU 106), a frequent and non-specific OTU, showed a sensitive profile to all the coatings but only at Lorient. Among the Bryozoa (only reported at Toulon), two OTUs were resistant to Z and I (OTU 121 and 124, respectively) whereas the third one (OTU 125) was sensitive to all the coatings. Finally, Cnidaria were noticed nearly exclusively at Lorient with complex sensitivity profiles similar to those found in Arthropoda.

Figure 5. Heatmap showing the resistant and sensitive Operational Taxonomic Units (OTUs) for each coating at each site. A ratio between the relative abundance of each OTU (i.e. mean of the four seasons) for C, Z or I and R at each site was calculated. Four categories were determined: ratio <0.1 very sensitive (bright red), $0.5 <$ ratio < 0.1 sensitive (dark red), $2 <$ ratio < 10 resistant (dark yellow), ratio > 10 very resistant (bright yellow). L = Lorient, T = Toulon. R = reference plates with no coating, I = plates coated with commercial binder (Neocryl® B-725) and Zineb®, C = plates coated with commercial binder (Neocryl® B-725) and copper pyrithione, Z = plates coated with commercial binder (Neocryl® B-725) and zinc pyrithione.

Structural variability - Visual analysis of biofouling coverage

Visual inspection undertaken on Toulon panels identified six major types of biofoulers: biofilm, Phaeophyceae (brown algae), Chlorophyceae (green algae) and Rhodophyceae (red algae), tubeworms, which are calcareous worms including mainly Annelida, and other hard fouling, mainly Bryozoa or barnacles (Figure 6). The PCA plot clearly showed that I coatings did not differ markedly from R panels (Figure 6). In contrast, C and Z coatings clustered together taking all the seasons into account and had less macrofouling, except in spring. The PERMANOVA analysis performed on percentage cover data indicated a significant effect of AF coating and season (Table 3). The pair-wise test of the AF coating showed marginally significant differences between R, I and C coatings (Table 3).

In terms of seasonal patterns, brown algae were dominant on R panels in autumn and winter, whereas green algae were dominant in spring and summer. Hard fouling was reported mostly in spring and mainly consisted of bryozoans and tube worms. R panels were consistently overgrown across seasons with various groups depending on the season.

Metabolomics analysis

The first PLS-DA score plot obtained from LC-MS data demonstrated a clear separation between samples collected from the two sites (Figure 7a). The corresponding PLS-DA model was well-fitted to the experimental data (Figure 7d) and consisted of four components, with the first dimension showing a significant separation between Toulon and Lorient samples. When considering only coatings, the samples were discriminated at each site depending on the type of biocide applied (Figure 7b and 7c). Among the PLS-DA models, those with three classes (one composed by C samples, another by R samples and a last class containing I and Z samples) gave better quality parameters than those constructed with four classes (one for each biocide) (Figure 7d). Moreover, for each site separately

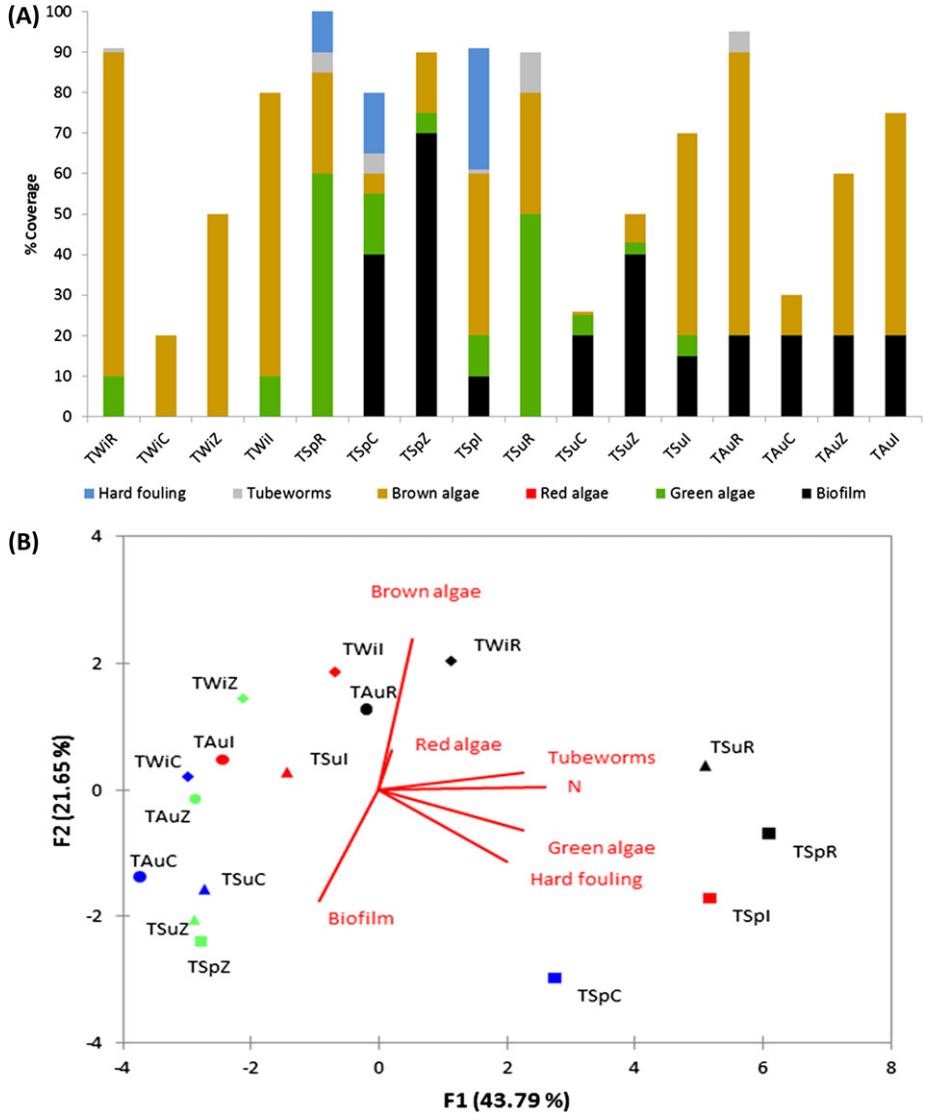

Figure 6. Relative abundance of the main groups of macrofoulers visually identified at Toulon (A), and the corresponding Principal Component Analysis (B). T = Toulon, Winter = Wi, Spring = Sp, Summer = Su, Autumn = Au. R = reference plates with no coating, I = plates coated with commercial binder (Neocryl® B-725) and Zineb®, C = plates coated with commercial binder (Neocryl® B-725) and copper pyrithione, Z = plates coated with commercial binder (Neocryl® B-725) and zinc pyrithione.

Table 3. PERMANOVA table for the multivariate effects of AF treatment and season on the biofouling community (cover percentage data from visual analysis at Toulon) and pair-wise test results for AF treatment factor.

PERMANOVA table of results						
Source	df	SS	MS	Pseudo-F	P(perm)	Unique perms
AF treatment	3	5302.1	1767.4	5.1957	0.003	9946
Season	3	9122.3	3040.8	8.9393	0.0002	9955
Residual	9	3061.4	340.2			
Total	15	17486				
Pair-wise tests for antifouling treatment						
Groups	t	P(MC)	Unique perms			
R, C	2.39	0.077	425			
R, Z	2.29	0.079	425			
R, I	3.52	0.048	425			
C, Z	1.51	0.198	425			
C, I	3.11	0.042	425			
Z, I	1.36	0.249	425			

Permutational (permutation of residuals under a reduced model) and Monte-Carlo (for location factor with low final number of permutations) *p* values applied to test for significance. R = reference plates with no coating, I = plates coated with commercial binder (Neocryl® B-725) and Zineb®, C = plates coated with commercial binder (Neocryl® B-725) and copper pyrithione, Z = plates coated with commercial binder (Neocryl® B-725) and zinc pyrithione.

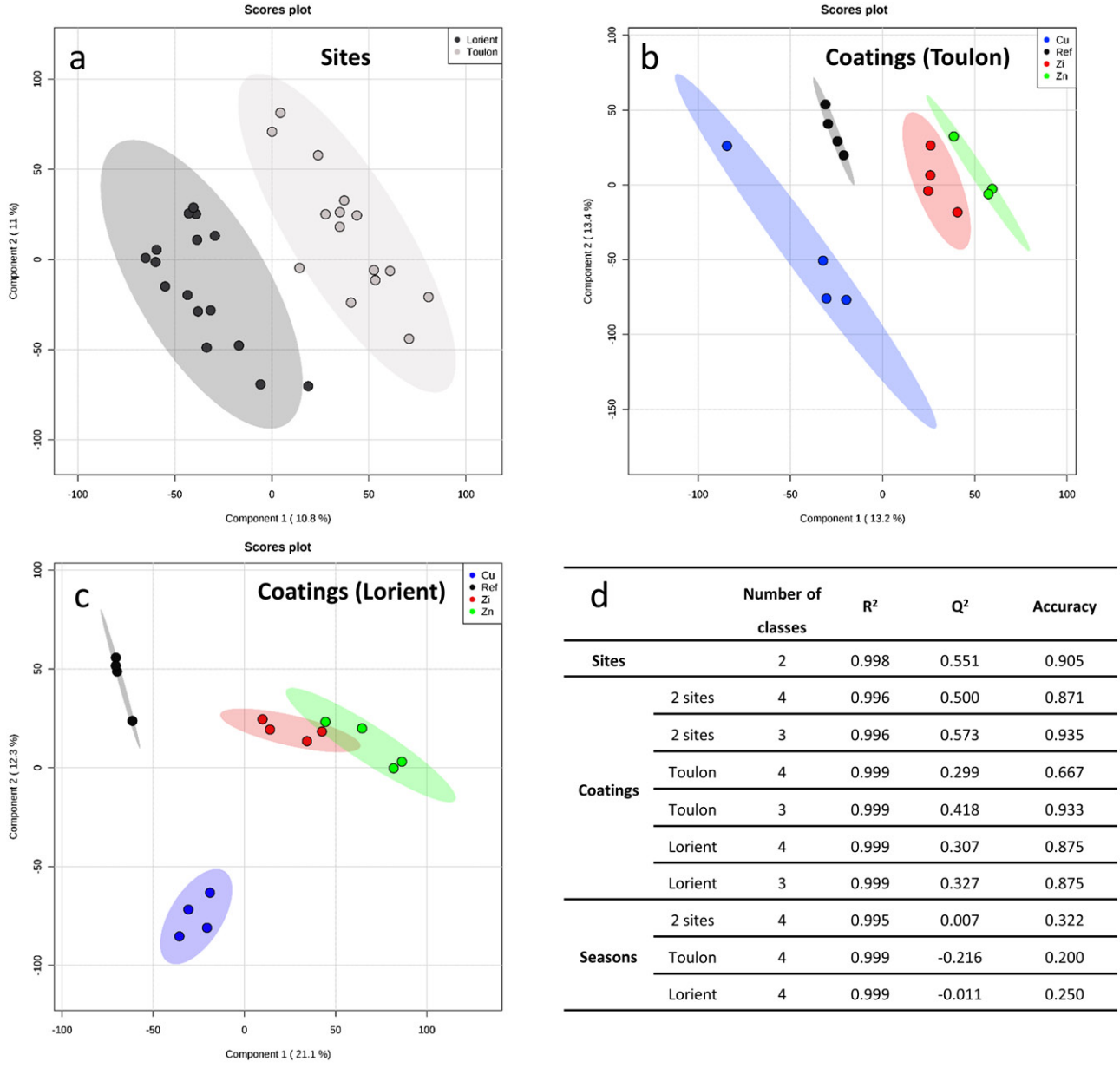

d

		Number of classes	R^2	Q^2	Accuracy
Sites		2	0.998	0.551	0.905
Coatings	2 sites	4	0.996	0.500	0.871
	2 sites	3	0.996	0.573	0.935
	Toulon	4	0.999	0.299	0.667
	Toulon	3	0.999	0.418	0.933
	Lorient	4	0.999	0.307	0.875
	Lorient	3	0.999	0.327	0.875
Seasons	2 sites	4	0.995	0.007	0.322
	Toulon	4	0.999	-0.216	0.200
	Lorient	4	0.999	-0.011	0.250

Figure 7. PLS-DA (Partial Least Squares regression – Discriminant Analysis) scores plot of liquid chromatography-mass spectrometry profiles of the biological material scraped from the artificial surfaces for comparison between the Toulon and Lorient sites (a) and coatings at Toulon (b) and Lorient (c). Statistics associated to the PLS-DA models are provided (d).

or in combination, this metabolomics approach did not show any significant discrimination between samples according to season (Figure 7d).

Meta-omics analyses

Canonical correspondence analysis was performed to assess if macrofouling taxa determined by HTS were associated to LC-MS profiles for the different coatings at both sites (Figure 8). The cumulative percentage of variance of the taxa (Class level)/metabolome relationship indicated that the first and second canonical axis explained 40.9% and 17.2% of the variance at Toulon, and 33.9% and 15.0% at Lorient, respectively (Figure 8). No clear trend could be observed at Toulon except for the relationship between metabolomes obtained from R panels immersed in spring and Bryozoan. Conversely, regardless of season at Lorient, metabolomes from R panels seemed to be associated with Arthropoda, Bryozoa, Mollusca Nematoda and unclassified metazoans, whereas metabolomes obtained from AF panels were related to Chlorophyta, Ciliophora, Cnidaria and Dinophyta.

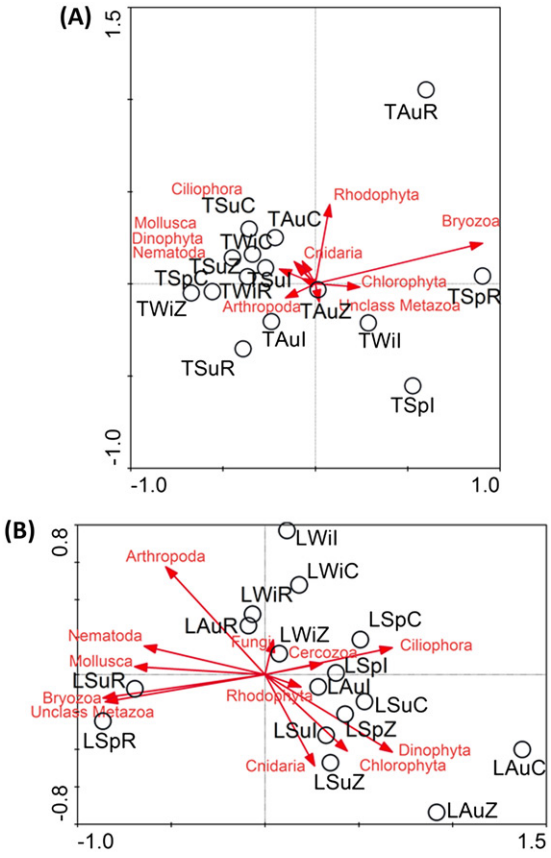

Figure 8. Canonical Correspondence Analysis (CCA) showing the relationship between macrofouling taxa and the liquid chromatography-mass spectrometry profiles for each coating at Toulon (A), and Lorient (B). L = Lorient, T = Toulon. R = reference plates with no coating, I = plates coated with commercial binder (Neocryl® B-725) and Zineb®, C = plates coated with commercial binder (Neocryl® B-725) and copper pyrithione, Z = plates coated with commercial binder (Neocryl® B-725) and zinc pyrithione.

Discussion

Improved knowledge on drivers of temporal and spatial shifts in eukaryotic biofouling communities can be obtained using recent technological advances such as metabarcoding and metabolomics. Metabarcoding is a powerful method for investigating taxonomic diversity at high resolution whereas metabolomics aims to characterize a wide range of metabolites (i.e. molecules with a molecular mass lower than 1,500 Da). This study constitutes, to our knowledge, the first application of an approach combining both techniques to study marine biofouling communities. The visual determination of coverage (depending on groups determined at a very high taxonomic level) provides a complementary quantitative perspective of the macrofouling assemblages.

Environmental drivers of the macrofouling patterns

Eukaryotic communities detected from the panels differed between study sites, both in terms of community and metabolic profiles. Although they are both located in temperate areas, detected high beta-diversity is most likely explained by variations in environmental conditions between the Toulon and Lorient sites (Briand et al. 2017). The Lorient site is characterized by eutrophication, and lower and fluctuating salinities due to river inputs (Blavet River). Freshwater inflow probably also influences the nature and content of the dissolved organic matter. However, a previous study from an Irish marina suggested that the potential impact of freshwater input was limited on fouling assemblages (Saloni & Crowe 2015). Toulon harbour is characterized by environmental features typical for the Mediterranean coasts, such as high temperature and salinity, and the site is considered mesotrophic. In addition, the plate deployment site was located in a semi-enclosed basin with a very stable water column and a reduced input of the Ligurian-Provençal current. Both harbours are exposed to high metal contamination (mainly Cu and Zn) with especially high Pb contamination at Toulon dating back to World War II (Dang et al. 2015). Due to the freshwater inputs, resuspension of sediments is likely higher at Lorient compared to Toulon, which could increase the exposure of fouling communities to metals.

Conclusions similar to the current findings were previously drawn for prokaryotic communities settled on the same set of panels (Briand et al. 2017). However, the dissimilarity between the two sites on the R panels was clearly higher for eukaryotic assemblages (this study), compared to the prokaryotic communities reported earlier (59.8% *vs* 18.5% of dissimilarity; SIMPER analysis). Diatom communities, which were not amplified with the primers used here and consequently not considered in this work, have been previously studied with a classic microscopic approach (Briand et al. 2017) Interestingly, these communities showed an intermediate level of dissimilarity (41.8%). Consequently, the clear site discrimination observed by metabolomics is most likely linked to eukaryotes rather than prokaryotes. However, we can't exclude that similar prokaryotic taxa, adapted to dissimilar environments, exhibited different functions (Louca et al. 2016).

Taxonomic diversity of macrofouling community

Alpha diversity of eukaryotic assemblages was markedly lower than that of prokaryotic communities

(Briand et al. 2017), which is consistent with a previous similar study of biofouling using HTS (Zaiko et al. 2016). In addition, Toulon assemblages were less diverse compared to those found in Lorient, which also corresponds with the lower cover rate of the panels by biofoulers as reported by (Antoniadou et al. 2011).

Both sessile and motile eukaryotes were identified. This implies that sequenced communities could also include organisms associated with algae, such as the copepod *Harpacticus* sp., which constituted the most abundant taxa based on sequence reads number. In some cases, the high-level taxonomic assignment didn't allow us to draw any conclusions on specific biological traits. For example, one of the most abundant OTUs (OTU 115) could only be attributed to Maxillopoda that includes both motile copepods and sessile barnacles. Among the unicellular and highly diverse Ciliophora group, sessile (mainly *Zoothamnium* spp. and Vorticellidae from the order Sessilida), vagile (Hypotrichia) but also planktonic (Chloreotrichia) taxa were identified in this study. The diversity of vagile taxa has previously been reported to be linked to the increasing complexity of the habitat associated with the development of algae or sessile organisms (Antoniadou et al. 2011). A possible associative relationship can be inferred from the Dinophyceae observed in the Lorient samples. They are known as epibionts of Ulvophyceae, and are rarely reported among photosynthetic microorganisms on artificial substrata (e.g. Railkin, 2004). The present study revealed that dinoflagellates most commonly co-occurred with green algae, as shown by both visual inspections and metabarcoding data. The high diversity of Ciliates recorded at Lorient could also follow the development of algae, which increased the complexity of the habitat.

Eukaryotic communities exhibited site specificity at different taxonomic levels. If Arthropoda or Nematoda included both common (OTUs 106, 115, 153 and 154) and specific taxa (OTUs 98, 104, 118, 166 and 172 at Toulon *vs* OTU 101 at Lorient), Ciliophora (Phylum) or Ulvophyceae (Class) appeared to be specific to Lorient. Based on the combined results from visual assessment and metabarcoding, Toulon assemblages were dominated by Nematoda and Arthropoda in addition to the unamplified Ochrophyta. Nematodes are known to play an important role in the decomposition processes and the recycling of nutrients in marine environments. The hard fouling identified visually in spring at Toulon could be attributed to several Bryozoa taxa detected by metabarcoding (OTUs 119 to 125), that did not emerge as site-specific OTUs as they were also found at Lorient. Bryozoans have often been reported in biofouling assemblages in ports and marinas (Turner et al. 1997). Calcareous tubeworms revealed by macroscopic analyses at Toulon, except in winter, could be attributed to *Hydroides* sp., *Pileolaria* sp. (Serpulidae) or an unclassified Annelida, all of which being detected using metabarcoding. They are sessile, tube-building annelid worms of the class Polychaeta. Members of this family (also called spirorbids) secrete tubes of calcium carbonate and many of them bore into rock before doing so. Issues associated with DNA extraction from calcareous organisms could explain underrepresentation of these taxa in molecular data as it has also been previously suggested (Zaiko et al. 2016). Similar fouling communities were reported from panels immersed in the Aegean Sea (Eastern Mediterranean Sea, Greece) with dominant filamentous algae coexisting with small-sized serpulids and colonial bryozoans (Antoniadou et al. 2011).

Ulvophyceae are well-known indicators of eutrophication (e.g. Li et al. 2017) and, in the present study, distinguished the biofouling communities identified at Lorient and Toulon (metabarcoding and visual analysis). Ciliates (Ciliophora) were reported exclusively from the Lorient samples, and were dominated by *Zoothamnium* spp. and Vorticellidae. Similar taxonomic composition of the ciliate assemblages was recorded in the temperate state of Victoria in Australia with a microscopic approach (Watson et al. 2015b). The fact that ciliates were not detected at Toulon, despite having extremely high rDNA gene copy numbers among protists (Gong et al. 2013), may partly explain the higher densities of prokaryotes already reported at Toulon compared to Lorient in Briand et al. (2017), due to reduced grazing pressure. Sessile hydrozoans that belong to Cnidaria (*Clytia hemisphaerica,* OTU 128, *Ectopleura larynx*, OTU 130 and *Gonothyraea loveni*, OTU 133) have also contributed to the high diversity recorded at Lorient.

Seasonal patterns in macrofouling assemblages

The higher seasonal taxonomic variability at Lorient could be related to fluctuating conditions, especially associated with inflows of the Blavet River. Conversely, high levels of metal contamination at Toulon, in combination with low seasonal variations, could result in the formation of temporally stable assemblages, characterized by comparatively lower

diversity and dominated by metal-tolerant organisms. The low seasonal variability of the assemblages at Toulon could also indicate that, at this location, assemblages were able to converge within one month. Indeed, mature stages tend to converge into similar structures as biofouling succession progress (Antoniadou et al. 2011).

Seasonal metabolic diversity appeared to be low at the two sites and consequently partly divergent from metabarcoding taxonomic diversity, especially at Lorient. As already discussed, the metabolome could be composed of metabolites from both prokaryotes and eukaryotes, and the former exhibit low seasonal fluctuations (Briand et al. 2017). Moreover, such discrepancy can also be explained by underrepresentation of some functionally important taxa not reported in the metabarcoding dataset (e.g. Chlorophyta and Ochrophyta). Limited quantitative capacity of metabarcoding (e.g. Sun et al. 2015) does not allow for accurate measurement of intraspecific spatio-temporal variations related to shifts in species abundances. Functional redundancy in some groups with high OTU diversity (e.g. Ciliophora or Cnidaria at Lorient) could also contribute to discrepancies in seasonal patterns derived from metabolomics and metabarcoding. Consequently, the meta-omics analyses performed here showed no relationship between metabarcoding and metabolomic in terms of seasonal shift regardless of site.

Summer and autumn samples exhibited higher taxonomic diversity at both sites, consistent with reported trends in bacterial communities from the same samples (Briand et al. 2017). A clear seasonal shift was observed at Lorient for two dominant phyla. Hydrozoans (Cnidaria) increased from winter to summer, with an apparent succession of some OTUs: *Gonothyraea loveni* (OTU 133) was more abundant in winter and spring, gradually substituted by *Clytia hemisphaerica* (OTU 128) and *Ectopleura larynx* (OTU 130) in summer. Ciliates, especially Zoothamniidae and Vorticellidae, were more predominant in summer and autumn with a drastic increase in abundance in autumn samples. Environmental factors other than water temperature, previously identified as a key driver (Watson et al. 2015b), might be responsible for these shifts at Lorient, as the highest diversity in autumn corresponded to a significant water temperature decrease in comparison to summer.

Responses of the macrofouling assemblages to antifouling coatings

As both sites were multi-contaminated, the corresponding benthic communities could be considered to be at least partially adapted to high metal concentrations. For example, a gradient of Cu and Zn levels has been shown to drive epifaunal communities in two New Zealand boat mooring areas (Turner et al. 1997). This could partly explain the fact that biocidal coatings used in the present study had less impact on eukaryotic assemblages compared to spatial effects, the opposite to the pattern observed conversely in prokaryotic and also diatom communities from the same samples (Briand et al. 2017). This limited impact could also be linked to low biocide concentrations in coatings (5% compared to 10 to 15% for booster biocides and up to 50% of copper in commercial coatings), which limited the microbial communities during a one-month immersion (Briand et al. 2017), but failed to prevent macrofouler settlement during the same time. Panels with the same coatings immersed for a one-year period confirmed the current findings with similar macrofouling assemblages observed for all panels, including the controls (data not shown).

Combining two meta-omics approaches, i.e. metabarcoding and metabolomics, can improve knowledge of complex biological systems such as marine biofouling assemblages. In the CCA analysis, taxonomic groups (phyla) derived from metabarcoding were used as independent variables for explaining the clustering of the samples based on their metabolomic profiles. This approach provided insights on the functional biodiversity associated with the studied experimental factors. The analysis showed the two sites clearly diverged in relation to the AF treatments. At Lorient, two distinct groups of taxa, associated either with R panels or AF coatings, could be related to the particular metabolic profiles. The use of high resolution mass spectrometry will enable further progress to be made in identifying the molecular marker of metal resistance in the future.

The apparent contradiction between the taxonomic and metabolic data could also be partly associated with the use of the presence/absence Jaccard index for HTS-based community analysis. Such an approach, although considered more conservative and appropriate when dealing with imperfect precision in absolute quantification of 18S rDNA gene based metabarcoding data, does not allow the highlighting of quantitative variation in OTUs. In some cases, taxonomic affiliation may also lack precision when trying to decipher transition states from sensitive to resistant taxa within the same genus or family. Finally, intraspecific selection of resistant variants, or AF-specific

functional response of the same species, could also partly explain similar community composition.

However, metabarcoding results allowed determination of the taxa containing OTUs, which have demonstrated either resistance or sensitivity to applied biocides. Although some taxa, such as the Arthropoda and Cnidaria, seemed to be sensitive to one biocidal coating but resistant to another, global trends could be determined. There are previous studies demonstrating partially coherent results with the present findings, especially the various tolerance levels of invertebrates at the genus/species level (e.g. Neira et al. 2014, von Ammon et al. 2018). Ciliates were also reported to be selected at the surfaces of AF paints without noticeable taxonomic based trends (Watson et al. 2015a). However, inconsistent taxonomic resolution achieved by conventional morphological identification and lack of information on the ecotoxicity for most of the marine macrofoulers, makes comparison with previous data and further generalizations difficult.

Challenges of using high-throughput sequencing for describing taxonomic diversity of a macrofouling community

Although metabarcoding has proven to be a powerful tool for biodiversity studies and increasingly used in environmental research, there are still some caveats regarding its application and interpretation of the results from biofouling communities. The authors believe it is important to honestly describe current limitations, delineating existing challenges as well as highlighting avenues for future research and improvements. Given the high eukaryotic diversity in marine biofouling, the major challenge of biodiversity assessment using metabarcoding is to select universal primers. The primers used in this work targeted the hypervariable V4 region of the small subunit ribosomal DNA that displays a good coverage of major invertebrate groups of Crustacea, Mollusca and Tunicata (Zhan et al. 2013). The coverage of the Metazoans determined for these primers *in silico* using the SILVA database reached 86% (Quast et al. 2013). High coverage was also found for additional relevant taxonomic groups such as Ciliophora (72%), Alveolata (74%) (including the Dinophyceae 86%), but also the main groups of algae involved in biofouling, i.e. Chlorophyta (81%) or Rhodophyta (89%). However, Chlorophyta did not seem to be successfully amplified from Toulon samples, even though they were macroscopically identified on the panels (Figure 6). Although Ulvophyceae were abundant at Lorient (Bressy et al. 2014), they did not yield high percentages of the amplified sequences. Additionally, in the *in silico* test of the 18S V4 primers, Ochrophyta (brown algae) was poorly represented in the metabarcoding data (0.7%). Therefore, it is suggested that for reliable representation of eukaryotic autotrophs using metabarcoding on biofouling samples, the protocol should be optimized, e.g. by adjusting DNA extraction procedures and by targeting multiple markers especially those that specifically target plants and algae (e.g. *tuf*A, *rbc*L (Kress & Erickson 2007, Sauvage et al. 2016).

Acknowledgments

The authors wish to thank S. Lafond for her help in paint formulation, surface painting and contact angle measurements and Dr A. Ortalo-Magné (MAPIEM, UTLN) for helpful discussions and sample treatment for the metabolomics analysis. This work was funded by a grant from the French EC2CO program ANTECOL.

Disclosure statement

No potential conflict of interest was reported by the authors.

ORCID

Jean-François Briand http://orcid.org/0000-0001-8729-2621
Gérald Culioli http://orcid.org/0000-0001-5760-6394

References

Anderson MJ. 2001. A new method for non-parametric multivariate analysis of variance. Austral Ecol. 26:32–46.
Antoniadou C, Voultsiadou E, Chintiroglou C. 2011. Seasonal patterns of colonization and early succession on sublittoral rocky cliffs. J Exp Mar Biol Ecol. 403:21–30. doi:10.1016/j.jembe.2011.04.001
Bates D, Machler M, Bolker BM, Walker SC. 2015. Fitting linear mixed-effects models using lme4. J Stat Softw. 67:1-48.
Beale DJ, Barratt R, Marlow DR, Dunn MS, Palombo EA, Morrison PD, Key C. 2013. Application of metabolomics to understanding biofilms in water distribution systems: a pilot study. Biofouling. 29:283–294. doi:10.1080/08927014.2013.772140
Braithwaite RA, McEvoy LA. 2004. Marine biofouling on fish farms and its remediation. In: Advances in marine biology. London: Academic Press. London p. 215–252.
Brauer JI, Makama Z, Bonifay V, Aydin E, Kaufman ED, Beech IB, Sunner J. 2015. Mass spectrometric metabolomic imaging of biofilms on corroding steel surfaces using laser ablation and solvent capture by aspiration. Biointerphases. 10:019003. doi:10.1116/1.4906744

Bressy C, Briand J-F, Compère C, Réhel K. 2014. Efficacy testing of biocides and biocidal coatings: laboratory assays and field test evaluation method. In: Biofouling methods. Oxford, UK: Wiley-Blackwell. p. 332–345.

Briand J-F, Barani A, Garnier C, Réhel K, Urvois F, LePoupon C, Bouchez A, Debroas D, Bressy C. 2017. Spatio-temporal variations of marine biofilm communities colonizing artificial substrata including antifouling coatings in contrasted French coastal environments. Microb Ecol. 74:585–598. doi:10.1007/s00248-017-0966-2

Brown CJ. 2005. Epifaunal colonization of the Loch Linnhe artificial reef: Influence of substratum on epifaunal assemblage structure. Biofouling. 21:73–85. doi:10.1080/08927010512331344197

Brown CJ, Eaton RA, Cragg SM, Goulletquer P, Nicolaidou A, Bebianno MJ, Icely J, Daniel G, Nilsson T, Pitman AJ, et al. 2003. Assessment of effects of chromated copper arsenate (CCA)-treated timber on nontarget epibiota by investigation of fouling community development at seven European sites. Arch Environ Contam Toxicol. 45:37–47. doi:10.1007/s00244-002-0178-7

Camps M, Barani A, Gregori G, Bouchez A, Le Berre B, Bressy C, Blache Y, Briand J-F. 2014. Antifouling coatings influence both abundance and community structure of colonizing biofilms: a case study in the Northwestern Mediterranean Sea. Appl Environ Microbiol. 80:4821–4831. doi:10.1128/AEM.00948-14

Connell SD. 2001. Urban structures as marine habitats: an experimental comparison of the composition and abundance of subtidal epibiota among pilings, pontoons and rocky reefs. Environ Sci Technol 52:115–125.

Dang DH, Schafer J, Brach-Papa C, Lenoble V, Durrieu G, Dutruch L, Chiffoleau JF, Gonzalez JL, Blanc G, Mullot JU, et al. 2015. Evidencing the impact of coastal contaminated sediments on mussels through Pb stable isotopes composition. Environ Sci Technol. 49:11438–11448. doi:10.1021/acs.est.5b01893

Dürr S, Thomason JC. 2010. Biofouling. Wiley-Blackwell.

Edgar RC, Haas BJ, Clemente JC, Quince C, Knight R. 2011. UCHIME improves sensitivity and speed of chimera detection. Bioinformatics. 27:2194–2200. doi:10.1093/bioinformatics/btr381

Gong J, Dong J, Liu X, Massana R. 2013. Extremely high copy numbers and polymorphisms of the rDNA operon estimated from single cell analysis of oligotrich and peritrich ciliates. Protist. 164:369–379. doi:10.1016/j.protis.2012.11.006

Guillou L, Bachar D, Audic S, Bass D, Berney C, Bittner L, Boutte C, Burgaud G, de Vargas C, Decelle J, et al. 2013. The Protist Ribosomal Reference database (PR2): a catalog of unicellular eukaryote Small Sub-Unit rRNA sequences with curated taxonomy. Nucleic Acids Res. 41:D597–D604.

Gutarowska B, Celikkol-Aydin S, Bonifay V, Otlewska A, Aydin E, Oldham AL, Brauer JI, Duncan KE, Adamiak J, Sunner JA, et al. 2015. Metabolomic and high-throughput sequencing analysis—modern approach for the assessment of biodeterioration of materials from historic buildings. Frontiers Microbiol. 29:6.

Hanson CH, Bell J. 1976. Subtidal and intertidal marine fouling on artificial substrata in northern Puget Sound, Washington. Fishery Bulletin. 74:377–385.

Kelly RP, Port JA, Yamahara KM, Martone RG, Lowell N, Thomsen PF, Mach ME, Bennett M, Prahler E, Caldwell MR, et al. 2014. Environmental monitoring. Harnessing DNA to improve environmental management. Science. 344:1455–1456. doi:10.1126/science.1251156

Kozich JJ, Westcott SL, Baxter NT, Highlander SK, Schloss PD. 2013. Development of a dual-index sequencing strategy and curation pipeline for analyzing amplicon sequence data on the MiSeq Illumina sequencing platform. Appl Environ Microbiol. 79:5112–5120. doi:10.1128/AEM.01043-13

Kress WJ, Erickson DL. 2007. A two-locus global DNA barcode for land plants: the coding rbcL gene complements the non-coding trnH-psbA spacer region. PLoS One. Jun;2:10.

Leary DH, Li RW, Hamdan LJ, Hervey WJ, Lebedev N, Wang Z, Deschamps JR, Kusterbeck AW, Vora GJ. 2014. Integrated metagenomic and metaproteomic analyses of marine biofilm communities. Biofouling. 30:1211–1223. doi:10.1080/08927014.2014.977267

Li HM, Zhang YY, Tang HJ, Shi XY, Rivkin RB, Legendre L. 2017. Spatiotemporal variations of inorganic nutrients along the Jiangsu coast, China, and the occurrence of macroalgal blooms (green tides) in the southern Yellow Sea. Harmful Algae. 63:164–172. doi:10.1016/j.hal.2017.02.006

Louca S, Parfrey LW, Doebeli M. 2016. Decoupling function and taxonomy in the global ocean microbiome. Science. 353:1272–1277. doi:10.1126/science.aaf4507

Neira C, Levin LA, Mendoza G, Zirino A. 2014. Alteration of benthic communities associated with copper contamination linked to boat moorings. Mar Ecol-Evol Persp. 35:46–66. doi:10.1111/maec.12054

Oksanen J, Blanchet F, Kindt R, Legendre P, Minchin P, O'Hara R, Simpson G, Solymos P, Stevens M, Wagner H, et al. 2014. Vegan: community ecology package version 2.2-0. Available from: http://cranr-projectorg/web/packages/vegan/veganpdf.

Pochon X, Bott NJ, Smith KF, Wood SA. 2013. Evaluating detection limits of next-generation sequencing for the surveillance and monitoring of international marine pests. PLoS One. 8:e73935. doi:10.1371/journal.pone.0073935

Pochon X, Zaiko A, Hopkins GA, Banks JC, Wood SA. 2015. Early detection of eukaryotic communities from marine biofilm using high-throughput sequencing: an assessment of different sampling devices. Biofouling. 31:241–251. doi:10.1080/08927014.2015.1028923

Pramanik S, Li H. 2002. Direct detection of insertion/deletion polymorphisms in an autosomal region by analyzing high-density markers in individual spermatozoa. Am J Hum Genet. 71:1342–1352. doi:10.1086/344713

Quast C, Pruesse E, Yilmaz P, Gerken J, Schweer T, Yarza P, Peplies J, Glockner FO. 2013. The SILVA ribosomal RNA gene database project: improved data processing and web-based tools. Nucleic Acids Res. 41:D590–D596.

Railkin AI. 2004. Marine biofouling: colonization processes and defenses Boca Raton, Florida, US: CRC Press.

Saloni S, Crowe TP. 2015. Impacts of multiple stressors during the establishment of fouling assemblages. Mar Pollut Bull. 91:211–221. doi:10.1016/j.marpolbul.2014.12.003

Sanli K, Bengtsson-Palme J, Nilsson RH, Kristiansson E, Rosenblad MA, Blanck H, Eriksson KM. 2015. Metagenomic sequencing of marine periphyton: taxonomic

and functional insights into biofilm communities. Frontiers Microbiol. 6:1192.

Sathe P, Laxman K, Myint MTZ, Dobretsov S, Richter J, Dutta J. 2017. Bioinspired nanocoatings for biofouling prevention by photocatalytic redox reactions. Scientific Reports. 7:12.

Sauvage T, Schmidt WE, Suda S, Fredericq S. 2016. A metabarcoding framework for facilitated survey of endolithic phototrophs with tufA. Bmc Ecology. 16:21.

Schloss PD, Westcott SL, Ryabin T, Hall JR, Hartmann M, Hollister EB, Lesniewski RA, Oakley BB, Parks DH, Robinson CJ, et al. 2009. Introducing mothur: open-Source, platform-independent, community-supported software for describing and comparing microbial communities. Appl Environ Microbiol. 75:7537–7541. doi:10.1128/AEM.01541-09

Sun C, Zhao Y, Li H, Dong Y, MacIsaac HJ, Zhan A. 2015. Unreliable quantitation of species abundance based on high-throughput sequencing data of zooplankton communities. Aquat Biol. 24:9–15. doi:10.3354/ab00629

Taberlet P, Coissac E, Pompanon F, Brochmann C, Willerslev E. 2012. Towards next-generation biodiversity assessment using DNA metabarcoding. Mol Ecol. 21:2045–2050. doi:10.1111/j.1365-294X.2012.05470.x

Turner SJ, Thrush SF, Cummings VJ, Hewitt JE, Wilkinson MR, Williamson RB, Lee DJ. 1997. Changes in epifaunal assemblages in response to marina operations and boating activities. Mar Environ Res. 43:181–199. doi:10.1016/0141-1136(96)00086-4

von Ammon U, Wood SA, Laroche O, Zaiko A, Tait L, Lavery S, Inglis G, Pochon X. 2018. The impact of artificial surfaces on marine bacterial and eukaryotic biofouling assemblages: a high-throughput sequencing analysis. Mar Environ Res. 133:57–66.

Wang Q, Garrity GM, Tiedje JM, Cole JR. 2007. Naive Bayesian classifier for rapid assignment of rRNA sequences into the new bacterial taxonomy. Appl Environ Microbiol. 73:5261–5267. doi:10.1128/AEM.00062-07

Watson MG, Scardino AJ, Zalizniak L, Shimeta J. 2015a. Colonisation and succession of marine biofilm-dwelling ciliate assemblages on biocidal antifouling and fouling-release coatings in temperate Australia. Biofouling. 31:709–720. doi:10.1080/08927014.2015.1105221

Watson MG, Scardino AJ, Zalizniak L, Shimeta J. 2015b. Colonisation and succession of marine biofilm-dwelling ciliates in response to environmental variation. Aquat Microb Ecol. 74:95–105. doi:10.3354/ame01731

Wood CD, Truby K, Stein J, Wiebe D, Holm E, Wendt D, Smith C, Kavanagh C, Montemarano J, Swain G, et al. 2000. Temporal and spatial variations in macrofouling of silicone fouling-release coatings. Biofouling. 16:311–322. doi:10.1080/08927010009378454

Zaiko A, Schimanski K, Pochon X, Hopkins GA, Goldstien S, Floerl O, Wood SA. 2016. Metabarcoding improves detection of eukaryotes from early biofouling communities: implications for pest monitoring and pathway management. Biofouling. 32:671–684. doi:10.1080/08927014.2016.1186165

Zhan A, Hulak M, Sylvester F, Huang X, Adebayo AA, Abbott CL, Adamowicz SJ, Heath DD, Cristescu ME, MacIsaac HJ. 2013. High sensitivity of 454 pyrosequencing for detection of rare species in aquatic communities. Methods Ecol Evol. 4:558–565. doi:10.1111/2041-210X.12037